Theory for Radii and Second Virial Coefficients. 2. Weakly Charged Polyelectrolytes

Dirk Stigter and Ken A. Dill*

Department of Pharmaceutical Chemistry, University of California, San Francisco, California 94143

Received July 22, 1994; Revised Manuscript Received March 10, 1995®

ABSTRACT: We compare simple models for the radii of gyration and second virial coefficients of weakly charged polymers. In the preceding paper (paper 1) we found that highly charged chains are well modeled as flexible rods whose persistence length and effective width depend on linear charge density and ionic strength. Here we define a ratio of effective persistence length to effective chain width. When this ratio falls below 1, as for weakly charged polymers, coil radii and virial coefficients are better modeled as chains of beads, as in Flory–Huggins theory, than as chains of rodlike segments, as in many polyelectrolyte theories. For small coils of partially ionized chains, we also find it is important to account for the changing of ionization state of the monomers with radius, and we generalize a variational method of Sharp and Honig to treat this situation in terms of intrinsic pK's and solution pH.

1. Introduction

This is the second of two papers which develop theory for the radii of gyration and second virial coefficients (A_2) of polyelectrolytes. Paper 1[1] treats highly charged polyelectrolytes; here we consider weakly charged and ionizable polymers including proteins. We can distinguish between "highly" and "weakly" charged polyelectrolytes roughly as follows. When every monomers of a chain is charged, the charge density is usually sufficiently high that we call them highly charged. Examples include DNA and PSS; such cases were treated in paper 1. But when charge densities are lower, for example in polyelectrolyte copolymers containing some noncharged monomers, including proteins, or polymers in which the monomers are partially ionized due to solution pH, these constitute weakly charged polyelectrolytes. The latter are the subject of the present paper. In weakly charged molecules of a size commensurate with the Debye length of the solution, the degree of ionization of the monomers may vary with the radius of the chain and not be uniform. Such effects are of interest here. Our aim is to develop a theory that is simple enough that it will apply not only to expanded states, as are typically modeled in polyelectrolyte theories, but ultimately over the full range of compactnesses from very good to very poor solvents. Such approaches might ultimately be useful for proteins.

We compare two types of models: bead models, such as those used in Flory–Huggins theory, in which chains are modeled as strings of approximately monomer-sized beads, with charge interactions as in the Hermans–Overbeek polyelectrolyte theory,[2] and rod models, in which chains are modeled as connected rodlike segments, the lengths of which are determined by local charge and stiffness factors. In paper 1[1] we found that the model of uniformly charged connected rods (kinked rod model) gives good predictions of coil size and A_2 of highly charged polyelectrolytes. We have also found that the kinked rod and the bead models are about equivalent in predicting the chain size and second virial coefficient of uncharged polymers, provided the χ parameter for segment contact interactions is adjusted appropriately (Stigter and Dill, unpublished). In this paper we consider partially ionized polyelectrolytes.

Hermans and Overbeek[2] introduced the porous sphere model of polyelectrolytes with a uniform distribution of fixed charge over the chain volume. For proteins Stigter and Dill[3] used a similar model but generalized the treatment to allow the density of fixed charges on the chain to vary, depending self-consistently on the local electrostatic potential. In both cases the potential distribution was derived by integration of the linearized Poisson–Boltzmann (PB) equation, with a subsequent charging process leading to the electrostatic free energy of the system. The modified Hermans–Overbeek model predicts pH and salt effects on the folding of myoglobin very well, suggesting that this model is suitable for weakly charged polymers such as proteins. Here our aim is to compare the modified HO approach with the rod model of paper 1 and compare both to experiments.

There are several ways to evaluate the electrostatic free energy, F_{elec}, of polyelectrolyte models. Sharp and Honig[4] derived F_{elec} by a variational method. They considered charges fixed on the polyelectrolyte to be constant and not dependent on the field of the other charges fixed to the polymer. Since the variational method eliminates the charging process to obtain F_{elec}, it facilitates the use of the full (nonlinearized) PB equation. In this paper we extend the variational method to models in which the polyelectrolyte charges are themselves dependent on the surrounding electrostatic field, which is of importance for polyelectrolytes, including proteins, with partially ionized groups that can change ionization state.

We shall compare the above approaches with the charged rod model used in part 1. Of particular interest is the case of low charge and low molecular weight, in the range of those met in many proteins. An early treatment dealing with the second virial coefficient of polyelectrolytes is by Orofino and Flory.[5] They make two simplifying assumptions: constant coil size and shape, regardless of overlap, and they evaluate F_{elec} by means of the Donnan theory. We shall compare the Hermans–Overbeek results with the Donnan approach.

2. Bead Model with Uniform Segment Distribution and Hermans–Overbeek Electrostatics

Following Dill,[6] we model the polyelectrolyte molecule as a sphere with n/ϱ lattice sites over which the n

® Abstract published in *Advance ACS Abstracts,* July 1, 1995.

0024-9297/95/2228-5338$09.00/0

monomers are distributed randomly, the remaining $n/\varrho - n$ sites being occupied by solvent. ϱ is the coil density; its maximum value is $\varrho = 1$ when the chain is completely collapsed. The free energy of the single coil is given by

$$\frac{F_1}{kT} = -n\chi\varrho + n\left[\frac{1-\varrho}{\varrho}\ln(1-\varrho) + 1\right] + \frac{7}{2}\left(\frac{\varrho_0}{\varrho}\right)^{2/3} + 2\ln\frac{\varrho}{\varrho_0} + \frac{F_{elec}}{kT} \quad (1)$$

In eq 1 the first term is the contact free energy, where χ is the contact interaction parameter between "lattice monomers", the second term arises from (nonelectrostatic) excluded volume effects, the next two terms account for the elastic entropy of the polymer chain, given by the Flory–Fisk expression,[7] where ϱ_0 is the coil density in the Θ state (see eq 16 of paper 1), and F_{elec} is the electrostatic free energy per chain which is evaluated as in the Hermans–Overbeek porous sphere model of polyelectrolytes.[2]

The kinked rod model of paper 1[1] is based on the cylindrical symmetries in charge and potential distributions of individual rodlike segments within a chain molecule. A very different model arose much earlier from Hermans and Overbeek.[2] They treated polyelectrolyte chains as spheres of radius r_s with a constant fixed charge density throughout. Thus they exploited the global spherical symmetry of the whole molecule rather than the local cylindrical symmetry of a chain segment. Hermans and Overbeek assumed a linearized PB distribution of small salt ions inside and outside the coiled chain, with the uniform dielectric constant ϵ of water throughout. The electrostatic free energy of this uniform porous sphere with total fixed charge Ze is[2]

$$F_{elec} = \frac{3Z^2e^2}{4\pi\epsilon_0\epsilon r_s}\left\{\frac{1}{2x^2} - \frac{3}{4}\frac{x^2 - 1 + (1+x)^2e^{-2x}}{x^5}\right\} \quad (2)$$

where e is the protonic charge and ϵ_0 is the permittivity of vacuum. In eq 2 $x = \kappa r_s$ is a dimensionless quantity giving the sphere radius in units of the Debye length, $1/\kappa$, which is related to the molar concentration of univalent salt, M_{salt}, by

$$\kappa^2 = \frac{2e^2N_{av}M_{salt}}{1000\epsilon_0\epsilon kT} \quad (3)$$

The rms radius of gyration can then be evaluated using eq 1 and I-24. Unless stated otherwise, we assume no attraction between polyelectrolyte segments; that is, $\chi = 0$.

Orofino and Flory[5] applied a Donnan equilibrium treatment for the electrostatics based on local electroneutrality and, hence, a constant electrostatic potential inside the polyelectrolyte coil. Thus they neglect the microscopic details of how the electrostatic field or counterion distribution varies throughout the sphere. This model corresponds to the limit of the porous sphere model for high ionic strength,[2] that is, for $x = \kappa r_s \gg 1$. In this limit the first term in the braces in eq 2 dominates and we have:

$$\frac{F_{elec}}{kT} = \frac{3Z^2e^2}{8\pi\epsilon_0\epsilon kT\kappa^2 r_s^3} = -\chi_{elec}n\varrho \quad (4)$$

where we have expressed F_{elec} in terms of an electrostatic parameter χ_{elec} in the linear term in $n\varrho$ in eq 1. In the Orofino–Flory treatment,[5] the polymer volume may be expressed in terms of the site spacing of the cubic lattice, $d_{lattice}$ (Å)

$$V_{chain} = \frac{4}{3}\pi r_s^3\varrho = nd_{lattice}^3 \quad (5)$$

and the chain length is

$$L = nd_{lattice} \quad (6)$$

When each monomer contributes a charge αe to the total charge Ze per chain, and 2.49 Å to the chain length, eqs 3–6 give

$$\chi_{elec} = -\frac{66.9\alpha^2}{d_{lattice}M_{salt}} \quad (7)$$

3. Kinked Rod Model

In paper 1[1] we developed a rod model for polyelectrolyte radii and second virial coefficients. We follow the same treatment below, except that now, for weakly charged rods, we allow physical contact between chain segments. The contact interaction is given by a parameter X which is formally the same as the Flory–Huggins parameter χ in eq 1 but has a different value (see below) because X refers to a different model of the chain. Whereas χ is the short range interaction between two unconnected monomers on neighboring lattice sites, X is the (nonelectrostatic) interaction between two rods in contact. For each polymer molecule, the extra contact energy term is

$$\frac{F_{contact}}{kT} = -nX\varrho \quad (8)$$

The free energy per polyelectrolyte chain is now, instead of eq I-22,

$$\frac{F_1}{kT} = -nX\varrho + \frac{7}{2}\left(\frac{\varrho_0}{\varrho}\right)^{2/3} + 2\ln\frac{\varrho}{\varrho_0} + \frac{\pi}{4}\frac{L^2d_B}{V_{chain}}\varrho \quad (9)$$

where the volume of the chain with diameter d and length L is

$$V_{chain} = \frac{\pi}{4}d^2L \quad (10)$$

The geometry of the rod and bead models is related through eqs 5, 6, and 10. In the kinked rod model we assume the Flory–Fisk elastic entropy as in eq 1 for the bead model, but here we distinguish two charge effects: (i) The (local) repulsions between nearby charges along the chain are modeled in terms of a persistence length, the electrostatic contribution of which is interpolated from Le Bret's tables.[8] Thus local charge repulsions are accounted for in the reference density ϱ_0 through eqs I-14 to I-16. (ii) The (nonlocal) repulsion, due to steric and electrostatic interactions between segments that are distant along the chain, is treated in terms of the second virial coefficient between (relatively long) rodlike segments with effective diameter d_B, which may be larger than d due to the electrostatics. Details for highly charged rods are given in paper 1.[1] Here we summarize a treatment of d_B which is valid also for weakly charged rods with linear charge density ze.

A central quantity is the electrostatic contact potential W between perpendicular charged rods[9,10]

$$W = \frac{z^2e^2}{2\epsilon_0\epsilon kT\kappa}\frac{e^{-2x_0}}{[\beta\gamma x_0 K_1(x_0)]^2} \quad (11)$$

where $K_1(x_0)$ is a modified Bessel function of argument $x_0 = \kappa d/2$, and β and γ are factors that allow us to accurately represent the full nonlinear PB equation by using only the linearized version of it. These values approach $\beta = \gamma = 1$ for low potentials, that is for $W < 3$. In paper 1[1] we have called $ze/\beta\gamma$ the scaled rod charge density. Values of the scaling factor for B-DNA, $s_{rod} = 1/\beta\gamma$, are given in Table 1 of paper 1.[1] In the initial treatment of highly charged polyelectrolytes[9] the steric component of excluded volume played no role because the strong repulsion prevented significant contact between the rods. In that case

$$d_B = d + (\ln W + 0.7704)/\kappa \qquad \text{for } W > 3 \quad (12)$$

But for weakly charged rods eq 12 is no longer valid because the steric contribution to excluded volume becomes significant, and was treated by Fixman and Skolnick.[11] Using the numerical results of Fixman and Skolnick, valid for low W, d_B can be expressed[10] as a polynomial in W

$$d_B = d + (1.2634W - 0.4170W^2 + 0.1007W^3 - 0.0107W^4)/\kappa \qquad \text{for } W < 3.5 \quad (13)$$

In paper 1[1] we only used eq 12. In the following we use also eq 13, depending on the value of W.

We now relate the parameter X in eq 9 to χ in eq 1 by considering uncharged polymers. Then the last term of eq 9 becomes, with $d_B = d$, the chain cross-section $(\pi/4)d^2 = d^2_{lattice}$, and eqs 5, 6, and 10,

$$\frac{\pi}{4}\frac{L^2d}{V_{chain}}\varrho = \left(\frac{\pi}{4}\right)^{1/2} n\varrho = 0.886n\varrho \quad (14)$$

Substitution of eq 14 in eq 9 yields

$$\frac{F_1}{kT} = (-X + 0.886)n\varrho + \frac{7}{2}\left(\frac{\varrho_0}{\varrho}\right)^{2/3} + 2\ln\frac{\varrho}{\varrho_0} \qquad \text{uncharged rods} \quad (15)$$

For the uncharged bead model $F_{elec} = 0$ in eq 1, and in the limit of low density, when

$$n\left[\frac{1-\varrho}{\varrho}\ln(1-\varrho) + 1\right] = 0.5n\varrho \qquad \varrho \ll 1 \quad (16)$$

eq 1 becomes

$$\frac{F_1}{kT} = (-\chi + 0.5)n\varrho + \frac{7}{2}\left(\frac{\varrho_0}{\varrho}\right)^{2/3} + 2\ln\frac{\varrho}{\varrho_0} \qquad \text{uncharged beads, } \varrho \ll 1 \quad (17)$$

The difference between eqs 15 and 17 is the constant added to X or χ within the parentheses. In the low density limit, for uncharged polymers, eqs 15 and 17 have the same functional form. Then the rod and the bead models differ only in the interaction parameter: $-X + 0.886 = -\chi + 0.5$, or $X = \chi + 0.386$.

Table 1. Radius of Gyration, r_g, of Poly(acrylic acid), M = 770 000

				r_g, Å			
M_{NaCl}	α	P, Å	d_B, Å	HO	Donnan[a]	kinked rod[b]	exp[c]
0.10	0.102	9.4	12.2	513	515	529	560
1.00	0.947	15.1	14.0	716	717	604	670
0.10	0.335	14.2	27.2	744	747	671	720
0.10	0.959	26.7	38.2	1109	1112	832	750
0.01	0.344	39.3	109.0	1159	1168	1090	1080
0.01	0.994	65.3	132.0	1765	1774	1281	1240

[a] Most probable values. [b] rms values. [c] Orofino and Flory.[5]

4. Comparison of Theory with Experiments on Poly(acrylic acid)s

Orofino and Flory[5] have measured radii and second virial coefficients for poly(acrylic acid)s (PAA). Here we compare the three models to those experiments. Radii and second virial coefficients are obtained from the free energies by methods described in paper 1. We assume a contour length of 2.49 Å per monomer and a polymer density of 1 g/mL. This gives d = 7.82 Å for the diameter of the cylindrical chain in the rod model and $d_{lattice}$ = 6.93 Å for the size of a cubic lattice cell in the bead models. An intrinsic persistence length of 3.5 monomers[12] gives P_{intr} = 8.7 Å. The total persistence length, P, shown in Table 1, includes the electrostatic contribution interpolated from Le Bret's tables.[8] Unless noted otherwise, we neglect fluctuations; that is, we compute properties for the conformations that are at the minimum of the free energy, neglecting contributions from Boltzmann-weighted states near the free energy minimum.

Table 1 shows radii of gyration predicted from the Hermans–Overbeek[2] bead model (HO) with $\chi = 0$, from the Donnan approximation, and from the kinked rod model with $X = 0$, compared with experiments on a PAA sample of molecular weight M = 770 000. Since always $x = \kappa r_s \gg 1$, we find that the Donnan and the HO approch give nearly the same results, as expected since eq 4 approximates eq 2. In that case, the HO model predicts an electrostatic potential field that is nearly constant throughout the interior of the polyelectrolyte sphere, as assumed in the Donnan theory. The HO and Donnan models predict r_g's considerably higher than the experimental values (see Table 1, except the first row, which corresponds to a case of lower ionization).

On the other hand, the kinked rod model gives much better agreement with experiment. Root-mean-square values of r_g are shown in Table 1; they are obtained by using the predicted persistence lengths P and effective rod diameters d_B of poly(acrylic acid) in eq I-24 and eq 9 with $X = 0$ for the kinked rod model. Whereas these rms values take fluctuations into account, the most probable values of r_g (which neglect fluctuations, not shown in Table 1) obtained with eqs 9 and I-25 for the rod model are only 2–3% lower than the rms values.

Table 2 gives the corresponding comparison for the second virial coefficients, A_2, of poly(acrylic acid). Again the HO and the Donnan results are very close, and both predict second virial coefficients much higher than the experiments. The kinked rod model gives much better agreement. Allowing for mutual deformation of two approaching chains, whereby upon overlap each individual spherical chain can deform into an oblate ellipsoid, eq I-41 (neglecting fluctuations) leads to A_2

Table 2. Second Virial Coefficient, A_2, of Poly(acrylic acid), M = 770 000

			10^4A_2				
					kinked rod		
M_{NaCl}	α	W/kT	HO	Donnan	spheres	ellipsoids	exp[a]
0.10	0.102	0.41	23.8	24.0	23.4	12.2	5.95
1.00	0.947	3.57	83.1	83.4	31.6	18.0	10.0
0.10	0.335	3.46	95.2	96.3	49.5	25.2	22.2
0.10	0.959	10.8	372	375	82.5	46.0	43.9
0.01	0.344	12.9	432	443	206	107	69.5
0.01	0.994	27.4	1686	1713	293	166	196

[a] Orofino and Flory.[5]

values which are in reasonable agreement with the experiments. For the first entry in Table 2 the contact potential between crossed rods is only $W = 0.41kT$. This is low enough for frequent intersegment contacts which may be attractive. Accounting for such attraction with an extra χ term in the free energy would reduce the calculated A_2 value. The second entry in Table 2 is for 1 M NaCl, too high for reliable predictions based on the PB equation.

5. The Kinked Rod Model Applies to Stiff Chains

While we have concluded above that radii and second virial coefficients are best predicted by the kinked rod model, here we discuss its limitations. First note that the data in Table 1 present a puzzle. In principle, the kinked rod model ought to apply most appropriately when chain segments can be suitably modeled as rods, i.e., when the length of a segment is considerably greater than its diameter. But remarkably, Table 1 shows that the data of Orofino and Flory[5] cover a range in which the persistence length P is usually smaller than d_B; see also Figure 3. In this section, we describe a different quantity, the *effective* persistence length P_{eff}, which we believe is a more suitable measure of the appropriate rod length, which appears to allow a better rationalization of the data.

Before discussing this quantity, we describe how we will compare models throughout this section. Our interest in this section is just in the electrostatic contributions to the chain free energies, so we have matched the predictions of the HO and kinked rod models at degree of ionization α = 0 by adjusting the contact parameters to be $\chi = 0$ for the HO theory in eq 1 and $X = 0.386$ for the rod model in eq 9. With these values of the χ and X parameters, again we find in Figures 1 and 2, as in Tables 1 and 2, that the radii and second virial coefficients predicted by the HO theory are generally higher than for the rod model, particularly for large α. For small α, on the other hand, these differences become smaller or can, as shown in Figure 1 for 0.001 M salt, even reverse sign.

Now we focus on defining the lengths of the rod segments. For a short length l of the segment the (average) radius of curvature, R_c, is related to the change of direction, Θ, of the tangent to the chain by

$$R_c = 1/\Theta \tag{18}$$

A statistical treatment[13] relates Θ to the bending constant a of the chain. In terms of the persistence length, $P = a/kT$, for small l, we have

$$\Theta^2 = 2l/P \tag{19}$$

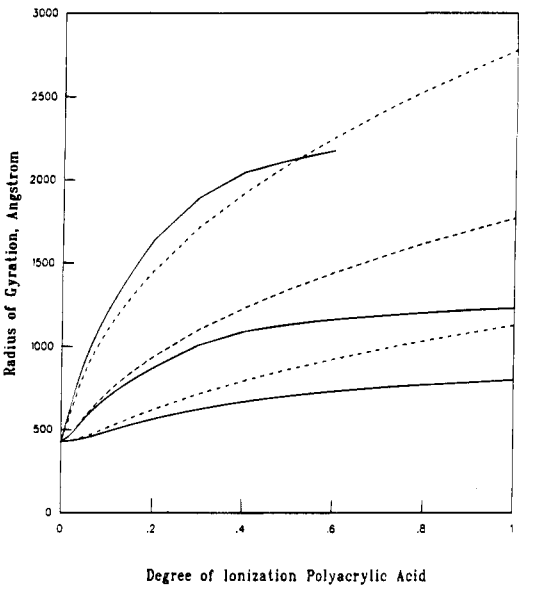

Figure 1. Radius of gyration of poly(acrylic acid) with molecular weight 770 000 as a function of degree of ionization. Solid curves: Kinked rod model. Dashed curves: Porous sphere model. Top to bottom: Ionic strength 0.001, 0.01, and 0.1 M.

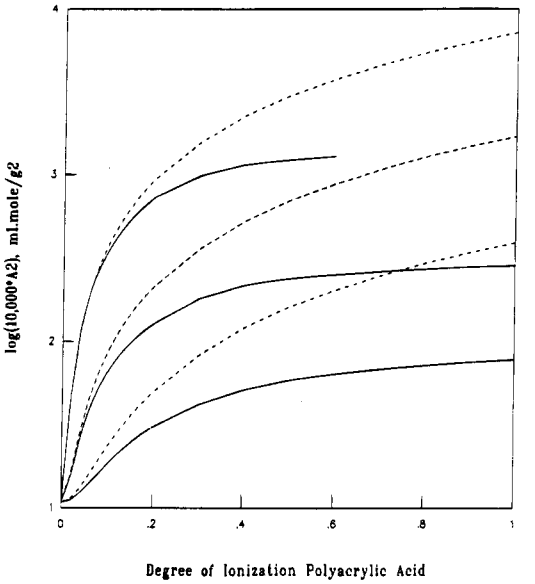

Figure 2. Second virial coefficient, A_2, of poly(acrylic acid) with molecular weight 770 000 as a function of degree of ionization. Solid curves: Kinked rod model. Dashed curves: Porous sphere model. Top to bottom: Ionic strength 0.001, 0.01, and 0.1 M.

or, with eq 18,

$$R_c^2 = lP/2 \tag{20}$$

If l is chosen to equal a persistence length, then eq 20 shows that R_c is also of order P.

But eq 19 was derived for noninteracting chains, that is, for polymers under Θ conditions. Polyelectrolytes, however, are expanded through electrostatic interactions. As a result the radius of gyration of the chain increases from the Θ value

$$(r_g)_0 = \left(\frac{PL}{3}\right)^{1/2} \tag{I-14}$$

to a larger value r_g, which defines an effective persis-

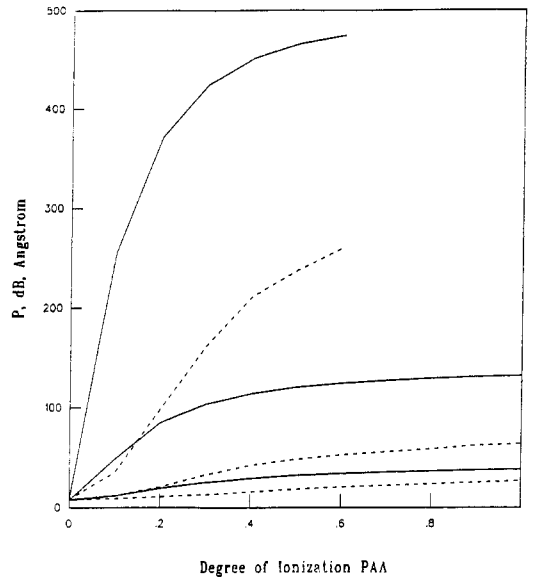

Figure 3. Effective diameter, d_B (solid curves), and persistence length, P (dashed curves), of poly(acrylic acid) with molecular weight 770 000 as a function of degree of ionization. Top to bottom: Ionic strength 0.001, 0.01, and 0.1 M.

Table 3. Ratio of Effective Persistence Length P_{eff} and Effective Diameter d_B of Poly(acrylic acid), M = 770 000

M_{NaCl}	α	P_{eff}/d_B
0.10	0.102	2.20
1.00	0.947	2.75
0.10	0.335	1.73
0.10	0.959	1.88
0.01	0.344	1.08
0.01	0.994	1.29

tence length P_{eff} through an identical equation

$$r_g = \left(\frac{P_{eff}L}{3}\right)^{1/2} \tag{21}$$

or

$$P_{eff} = 3r_g^2/L \tag{22}$$

This effective persistence length appears better able to rationalize agreement of the kinked rod model with experiments. Table 3 shows the ratio P_{eff}/d_B for the experiments of Orofino and Flory.[5] We suggest below that when P_{eff}/d_B becomes smaller than 1, the kinked rod model becomes poor, but it is greater than 1 for the data of Orofino and Flory, where we can therefore expect reasonable agreement of theory and experiment.

Figure 4 shows how P_{eff}/d_B depends on the ionic strength and on the degree of ionization, α, for the conditions in Figures 1–3, M = 770 000. It falls well below unity in 0.001 M salt solutions, just where the rod model predicts a larger radius than the HO theory (see Figure 1). The rod model is probably inappropriate here.

Should the kinked rod theory apply to proteins? Because the charges on proteins can be complex, here we consider a simpler experimental model system for comparison: we consider PAA with M = 20 000 and α from 0 to 0.1. This is in the range of size and charge density of small proteins. Figure 5 shows that the range of applicability of the kinked rod theory will strongly depend on the degree of ionization and salt concentration. It appears that for increasing repulsion between

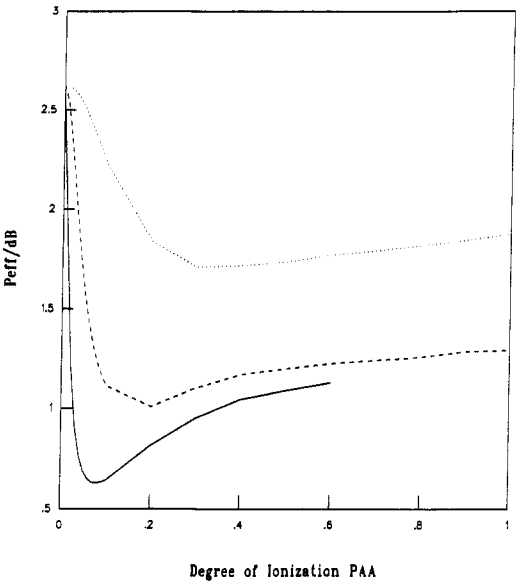

Figure 4. Ratio of effective persistence length, P_{eff}, and effective diameter, d_B, of poly(acrylic acid) with molecular weight 770 000 as a function of degree of ionization. Solid curve: 0.001 M ionic strength. Dashed curve: 0.01 M. Dotted curve: 0.1 M.

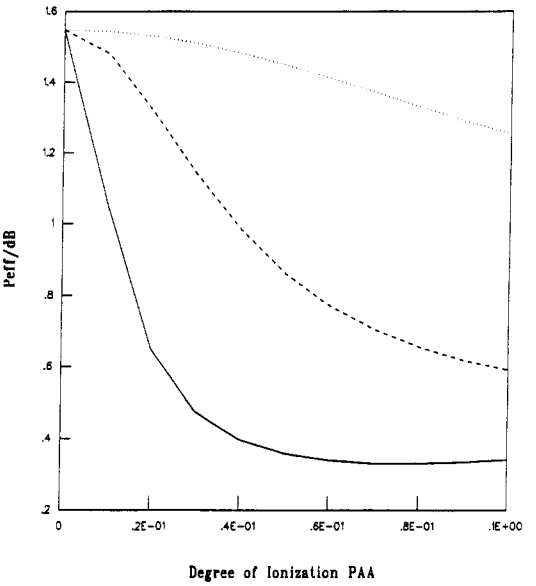

Figure 5. Ratio of effective persistence length, P_{eff}, and effective diameter, d_B, of poly(acrylic acid) with molecular weight 20 000 as a function of degree of ionization. Solid curve: 0.001 M ionic strength. Dashed curve: 0.01 M. Dotted curve: 0.1 M.

chain segments (increasing α and/or decreasing ionic strength) d_B increases relatively more than P_{eff}; compare also Table 3. In low salt (0.001 M), the kinked rod treatment will be a poor model since the chain is predicted to have very high curvature per unit chain diameter.

Figure 6 compares the radii of gyration predicted by HO and kinked rod models and shows that they are most different (by factor of about 2) in 0.001 M salt solutions, consistent with the expectation from Figure 5. Comparison of Figures 1 and 4 for M = 770 000 with Figures 5 and 6 for M = 20 000 shows that the validity of the kinked rod theory depends markedly on the polymer weight. This is not surprising. Chain curvature is decreased by excluded volume of the chain and this effect increases as L^2 (see eq I-22), that is, as M^2.

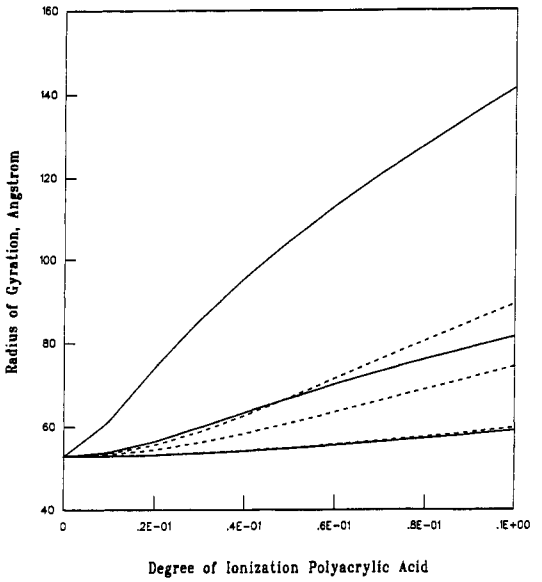

Figure 6. Radius of gyration of poly(acrylic acid) with molecular weight 20 000 as a function of degree of ionization. Solid curves: Kinked rod model. Dashed curves: Porous sphere model. Top to bottom: Ionic strength 0.001, 0.01, and 0.1 M.

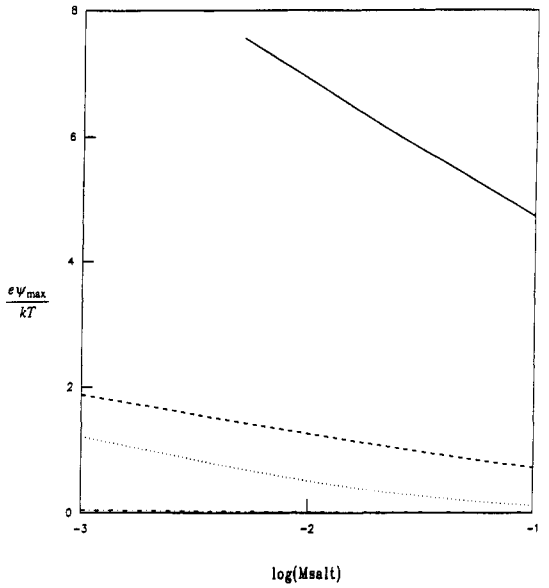

Figure 7. Maximum potential of poly(acrylic acid) chain models as a function of ionic strength. Solid curve: Kinked rod, degree of ionization $\alpha = 1$. Dashed curve: Kinked rod, $\alpha = 0.1$. Dotted curve: Porous sphere, $\alpha = 0.1$, polymer weight $M = 20\,000$. Dash–dotted curve: Porous sphere, $\alpha = 1$, $M = 770\,000$.

By this measure, short polymer chains are curved more strongly than long chains.

6. Would a Debye–Hückel Approximation Be Justified?

In this section, we consider the maximum value of the electrostatic potential field, ψ_{max}, which is a measure of the validity of the Debye–Hückel approximation to the PB equation. In the porous sphere model ψ_{max} is the potential at the center of the sphere, which in the HO model is (using the notation of eq 2)

$$\psi_{max} = \frac{3Ze}{4\pi\epsilon_0\epsilon r_s}\frac{1 - e^{-x}(1+x)}{x^2} \tag{23}$$

For the kinked rod treatment the potential is maximal at the surface of the rod where we have, using the notation of eq 11,

$$\psi_{max} = \frac{1}{\beta}\frac{ze}{2\pi\epsilon_0\epsilon}\frac{K_0(x_0)}{x_0K_1(x_0)} \tag{24}$$

Figure 7 shows ψ_{max} calculated from eqs 23 and 24 as a function of ionic strength for PAA with molecular weight $M = 770\,0000$ and degree of ionization $\alpha = 1$, and for $M = 20\,000$, $\alpha = 0.1$. For the rod model, ψ_{max} does not depend on M, but for the porous sphere model larger M gives lower chain density and, hence, lower potential. This dependence of ψ_{max} on M is strong. For example, Figure 7 shows that ψ_{max} for $\alpha = 0.1$, $M = 20\,000$ is much higher than for $\alpha = 1$, $M = 770\,000$. In general, the maximum potential of the porous sphere is considerably lower than for the rod because the charge in the sphere model is smeared over the entire chain volume instead of just at the surface of the polyelectrolyte rod. The extra smearing of the charge over the porous sphere reduces the extent and the peak values of the high potential region, and, therefore, the porous sphere is less sensitive to the effects of the nonlinearity of the full Poisson–Boltzmann equation. This is one reason that the predictions of the HO model for r_g and for A_2 are too high; another is that the electrostatic free energy of a smeared charge distribution contains self-energies of interactions among the charges. As a result eqs 2 and 4 give values for F_{elec} that are too high. In the kinked rod model this error is avoided because we consider only the repulsion between charged rods.

7. Other Models of the Electrostatic Free Energy

There are several ways to determine the electrostatic free energy, F_{elec}, of electrical double-layer systems. (i) We could start from screened Coulomb interactions between the charged particles of interest. This is the basis of the intersegment interaction in eqs 11, I-18, and I-20 of the kinked rod model. (ii) The PB equation could be solved for the potential field and used for determining the work in a charging process. This is the traditional method developed by Verwey and Overbeek[14] and used to obtain F_{elec} in eq 2 for the porous sphere.[2] We have taken this approach earlier for partially ionized polyelectrolytes.[3] (iii) More recently, several authors[4,15,16] have used a variational method to determine the free energy associated with the PB equation.

When used for the same model, the three different methods give equivalent results for F_{elec}, although often in different analytical form. Overbeek[17] has shown how to interconvert several different expressions for F_{elec} and how to separate F_{elec} into entropy and enthalpy contributions, and he has estimated the relative magnitudes of the various terms for some systems. Here we use the variational method to show how F_{elec} differs for polyelectrolytes and colloids with fixed charge (complete ionization) compared to systems with variable charge (partial ionization) on the polymer. These two cases have also different experimental applications: In fixed charge systems one may use the structural charge or the titration charge for the calculation of F_{elec}. But in variable charge systems it is more convenient and more accurate to use the intrinsic pK's of the ionizable fixed groups and the solution pH.

The variational method[18] uses the Euler–Lagrange equation to identify the minimum of the part of the free energy that is a function of the small ion distribution described by the PB equation. Reiner and Radke[15] have studied the validity of the variational approach to several electrical double-layer applications in considerable detail. Feller and McQuarrie[16] have combined the variational method and the hypernetted chain equation. Here we follow Sharp and Honig,[4] who start from the Euler–Lagrange equation to derive an expression for the electrostatic free energy, and we generalize it to treat cases of partial ionization.

In general, the electrostatic free energy of a chain, F_{elec}, can be expressed as a spatial integral over an electrostatic free energy *density*, F, which depends on Cartesian coordinates, on the local electrostatic (dimensionless) potential, $\phi = e\psi/kT$, and on its spatial derivatives, $\phi_x = \partial\phi/\partial x$, $\phi_y = \partial\phi/\partial y$, and $\phi_z = \partial\phi/\partial z$:

$$F_{elec} = \int F(x,y,z,\phi,\phi_x,\phi_y,\phi_z)\, dv \tag{25}$$

According to variational theory,[18] F_{elec} will be at an extremum (in this case a minimum) if the Euler–Lagrange equation holds for F:

$$\frac{\partial F}{\partial \phi} - \frac{\partial}{\partial x}\left(\frac{\partial F}{\partial \phi_x}\right) - \frac{\partial}{\partial y}\left(\frac{\partial F}{\partial \phi_y}\right) - \frac{\partial}{\partial z}\left(\frac{\partial F}{\partial \phi_z}\right) = 0 \tag{26}$$

Equation 26 is a second-order differential equation that applies to any free energy density. In the present case the free energy density of interest comes from the PB equation. To recognize the correspondence with eq 26 and anticipating that we shall express F_{elec} in units of kT, we write the PB equation as follows:

$$\frac{kT}{e}\varrho_f - \epsilon_0\epsilon\frac{k^2T^2}{e^2}\kappa^2 \sinh\phi + \epsilon_0\epsilon\frac{k^2T^2}{e^2}\left(\frac{\partial\phi_x}{\partial x} + \frac{\partial\phi_y}{\partial y} + \frac{\partial\phi_z}{\partial z}\right) \tag{27}$$

Separation of variables in F with

$$F = F_1(\phi) + F_2(x,\phi_x) + F_3(y,\phi_y) + F_4(z,\phi_z) \tag{28}$$

and comparing to eqs 26 and 27 lead to

$$\frac{dF_1}{d\phi} = \frac{kT}{e}\varrho_f - \epsilon_0\epsilon\frac{k^2T^2}{e^2}\kappa^2 \sinh\phi \tag{29}$$

$$\frac{\partial}{\partial x}\left(\frac{\partial F_2}{\partial \phi_x}\right) = -\epsilon_0\epsilon\frac{k^2T^2}{e^2}\frac{\partial\phi_x}{\partial x} \tag{30}$$

$$\frac{\partial}{\partial y}\left(\frac{\partial F_3}{\partial \phi_y}\right) = -\epsilon_0\epsilon\frac{k^2T^2}{e^2}\frac{\partial\phi_y}{\partial y} \tag{31}$$

$$\frac{\partial}{\partial z}\left(\frac{\partial F_4}{\partial \phi_z}\right) = -\epsilon_0\epsilon\frac{k^2T^2}{e^2}\frac{\partial\phi_z}{\partial z} \tag{32}$$

Considering the fixed charge density ϱ_f in eq 29 to be constant, independent of the electrostatic potential, the use of eq 28 and integration of eqs 29–32 give

$$F = \frac{kT}{e}\varrho_f\phi - \epsilon_0\epsilon\frac{k^2T^2}{e^2}\kappa^2 \cosh\phi - \epsilon_0\epsilon\frac{k^2T^2}{2e^2}(\phi_x^2 + \phi_y^2 + \phi_z^2) + C_1 + C_2(\phi_x + \phi_y + \phi_z) \tag{33}$$

If we set $F = 0$ for $\phi = 0$ everywhere, the integration constants are

$$C_1 = \epsilon_0\epsilon\frac{k^2T^2}{e^2}\kappa^2 \qquad C_2 = 0 \tag{34}$$

Using eq 3 for κ^2 and dividing eq 33 by kT yields with eq 25

$$\frac{F_{elec}}{kT} = \int\left[\frac{\varrho_f\phi}{e} - \frac{N_{av}M_{salt}}{1000}(2\cosh\phi - 2) - \epsilon_0\epsilon\frac{kT}{2e^2}(\phi_x^2 + \phi_y^2 + \phi_z^2)\right] dv \tag{35}$$

Equation 35 is the result of Sharp and Honig,[4] apart from errors of factors e and kT in some of the terms in their equation.

In the uniformly charged sphere model of polyelectrolytes ϱ_f is the constant and uniform density of the fixed charges given by

$$\varrho_f = \frac{3Z_e}{4\pi r_s^3} \qquad \text{for } r < r_s \tag{36}$$

$$\varrho_f = 0 \qquad \text{for } r > r_s$$

In this case of spherical symmetry, we apply eq 35 with the substitutions

$$\phi_x^2 + \phi_y^2 + \phi_z^2 = (d\phi/dr)^2 \text{ and } \int dv = \int_0^\infty 4\pi r^2\, dr$$

We now compare the approach of Sharp and Honig[4] to an earlier treatment of ours based on the HO model,[19] both of which have been applied to proteins. We assume that the fixed charge on the polymer derives from partially ionized acid and basic groups of type i, with concentration n_i and intrinsic proton binding constant $k_i = 10^{pK_i}$, in Langmuir adsorption equilibrium with the local proton concentration $H = 10^{-pH}e^{-\phi}$. The degree of ionization α_i of group i can then be written as

$$\alpha_i = \frac{s_i}{1 + s_i} \qquad s_i = 10^{q_i(pK_i - pH)}e^{-q_i\phi} \tag{37}$$

where $q_i = +1$ for basic and -1 for acid groups. The fixed charge density

$$\varrho_f = e\sum_i q_i\alpha_i n_i \tag{38}$$

is now a function of the potential ϕ through eq 37. Instead of eq 29 for constant ϱ_f, we now have

$$\frac{dF_1}{d\phi} = kT\sum_i q_i n_i \alpha_i(\phi) - \epsilon_0\epsilon\frac{k^2T^2}{e^2}\kappa^2 \sinh\phi \tag{39}$$

Using eq 37, the integration yields

$$F_1 = kT\sum_i n_i \ln(1 - \alpha_i) - \epsilon_0\epsilon\frac{k^2T^2}{e^2}\kappa^2 \cosh\phi \tag{40}$$

Now for spherical symmetry, instead of eq 35 we have

$$\frac{F_{elec}}{kT} = \int_0^\infty \left[\sum_i n_i \ln(1 - \alpha_i) - \frac{N_{av} M_{salt}}{1000}(2 \cosh \phi - 2) - \frac{\epsilon_0 \epsilon kT}{2e^2}\left(\frac{d\phi}{dr}\right)^2 \right](4\pi r^2)\, dr \quad (41)$$

An expression equivalent to eq 41 (numerically the same but of different analytical form) has been derived earlier through a different method, namely by a reversible charging process.[19] The variational method has some advantages over the charging method. In general, a charging process produces F_{elec} as an integral over the charging parameter λ, which runs from 0 to 1. Often this integration cannot be carried out analytically. Except for low potentials, the nonlinear PB equation yields an integrand which is nonlinear in λ. Therefore, to obtain F_{elec} by numerical evaluation of the charging integral, the nonlinear PB equation must be solved many times for values of λ between 0 and 1, a time-consuming procedure. On the other hand, results of the variational method, such as eqs 35 and 41, require the solution of the nonlinear PB equation only for the fully charged system (for $\lambda = 1$). In the special case of low potentials, when the PB equation may be linearized (DH approximation), the integrand of the charging integral is always proportional to λ, reducing the integration to $\int_0^1 \lambda\, d\lambda = {}^1/_2$. If, instead of the full PB equation we can use the DH approximation in eq 27, the factor 2 cosh ϕ − 2 in eqs 35 and 41 is replaced by ϕ^2. Using the DH approximation, eq 35 becomes

$$\frac{F_{elec}}{kT} = \frac{1}{2}\int_0^{r_s} \frac{\varrho_f \phi}{e}(4\pi r^2)\, dr \quad (42)$$

This is the expression used by Hermans and Overbeek[2] to obtain F_{elec} in eq 2.

Compared with eq 35, eq 41 also includes the (electrostatic part of the) binding free energy which is missing in the Sharp and Honig treatment of fixed charges.[4] In the polyelectrolyte sphere the relevant free energy density depends on the radial position r and is given by

$$-\varrho_f(r)\psi(r) + kT\sum_i n_i \ln(1 - \alpha_i(r)) \qquad \text{for } r < r_s \quad (43)$$

and vanishes outside the sphere. Here $\psi(r)$ is the potential difference between a free proton in the bulk solution and a proton bound to the polyelectrolyte at radial distance r. The second term in expression 43 derives from the entropy associated with a random distribution of protons over occupied and unoccupied adsorption sites with average $\alpha_i(r)$.

Equations 35 and 41 have a different standard state. When $\phi = 0$ everywhere, F_{elec} does not vanish in eq 41 as it does in eq 35. The residual quantity in eq 41 is

$$\frac{F_{elec}(\phi=0)}{kT} = \int \sum_i n_i \ln(1 - \alpha_i(\phi=0))\, dv \quad (44)$$

where $\alpha_i(\phi=0)$ is a function of pH as given by eq 37. This quantity cancels in studies of coil size or effects of ionic strength at constant pH—hence eq 35 is suitable in those cases—but studies of pH effects require it. Choosing between eq 35 and 41 will often depend on the available experimental input. If the titration charge is not known, one may use eq 41 with eq 37 for the α_i's.

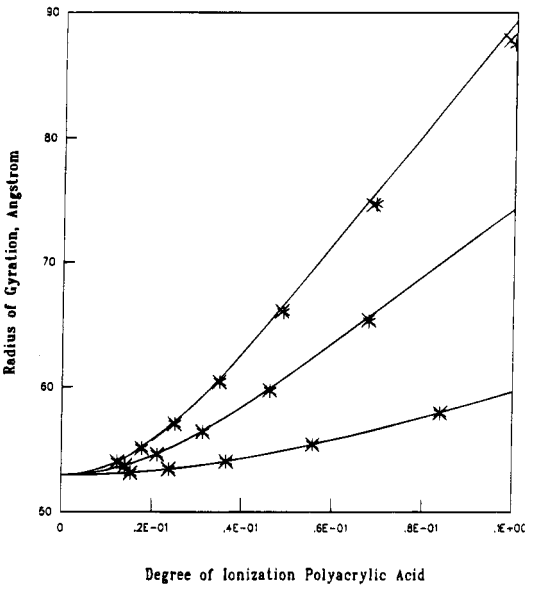

Figure 8. Radius of gyration of poly(acrylic acid) with molecular weight 20 000 as a function of degree of ionization for porous sphere models. Solid curves: Equation 2. (×): Equation 41 with full PB equation. (*): Equation 41 with DH approximation. Top to bottom: Ionic strength 0.001, 0.01, and 0.1 M.

On the other hand, if the polyelectrolyte charge is known experimentally and pK_i's are uncertain, one might use eq 35 with eq 36 for ϱ_f.

Figure 8 shows that the three different theories lead to nearly identical results for the radius of gyration of PAA with $M = 20\,000$, $\alpha = 0$–0.1. The solid curves are from eq 2 for the HO model with a constant, uniform, fixed charge density. The points are from eq 41 at various pH values and with self-consistent degrees of ionization $\alpha_i(r)$ from eq 37, with the full PB equation, and also with the DH approximation in eq 41. The differences among the results correlate with the potential fields in Figure 7 (dotted curve). For ionic strength 0.1 M there are no significant differences between the three sets of results. Here the potential in the porous sphere is so low that the radial variation of α_i is too small to have an effect on the term $n_i \ln(1 - \alpha_i)$. So the integral of this term does not depend on the chain density ϱ and we obtain the same chain size as with eq 35 or 2. In 0.001 M salt solutions the potential in the porous sphere may be of order $\phi = 1$; see Figure 7. Here the significant radial variation of ϕ is reflected in $\alpha_i(r)$, and as a result the relevant entropy influences F_{elec} in eq 41 as a function of the chain size. At the same time the DH approximation becomes less accurate, leading to differences between the two sets of points. Although the overall differences between the theories in Figure 8 are small, they indicate that for $\phi > 1$ the distributive entropy deriving from incomplete ionization begins to play a role, an effect that is missing in the Sharp and Honig treatment.[4] This conclusion applies not only in the present context but also to computing free energies of proteins with discrete ionic charges, where local potentials may be much higher than in the porous sphere model of smeared charges.

8. Conclusions

We consider polyelectrolytes that have partially ionized groups. When such polymers expand or contract, the ionization state of the monomers may change because of the different electrostatic potential that may

result. Examples include poly(acrylic acid)s and proteins. We study two models for the conformations and second virial coefficients of such polyelectrolytes: one in which the chain is represented as a string of rods, and the other in which the chain is a string of beads. As the degree of ionization increases, both models show chain expansion and increasing interchain repulsion. Whereas the persistence lengths of chains are normally defined in terms of the Θ state radius, we find here that an "effective" persistence length, compared with the effective chain diameter, is better able to rationalize the changeover in behavior from uncharged to highly charged chain behavior. We find that for low charge the ratio of the effective persistence length and the effective chain diameter decreases with increasing degree of chain ionization. We also generalize the variational derivation of Sharp and Honig[4] for electrostatic free energies to include partially ionized chains.

References and Notes

(1) Stigter, D.; Dill, K. A. *Macromolecules*, preceding paper in this issue (paper 1; eq x in paper 1 is denoted here eq I-x).
(2) Hermans, J. J.; Overbeek, J. Th. G. *Recl. Trav. Chim. Pays-Bas* **1948**, *67*, 761.
(3) Stigter, D.; Dill, K. A. *Biochemistry* **1990**, *29*, 1262.
(4) Sharp, K. A.; Honig, B. *J. Phys. Chem.* **1990**, *94*, 7684.
(5) Orofino, T. A.; Flory, P. J. *J. Phys. Chem.* **1959**, *63*, 283.
(6) Dill, K. A. *Biochemistry* **1985**, *24*, 1501.
(7) Flory, P. J.; Fisk, S. *J. Chem. Phys.* **1966**, *44*, 2243.
(8) Le Bret, M. *J. Chem. Phys.* **1982**, *76*, 6243.
(9) Stigter, D. *Biopolymers* **1977**, *16*, 1435.
(10) Stigter, D. *Macromolecules* **1982**, *15*, 635.
(11) Fixman, M.; Skolnick, J. *Macromolecules* **1978**, *11*, 863.
(12) Flory, P. J. *Statistical Mechanics of Chain Molecules*; Interscience: New York, 1969.
(13) Landau, L. D.; Lifshitz, E. M. *Statistical Physics*; Pergamon: Reading, MA, 1958.
(14) Verwey, E. J. W.; Overbeek, J. Th. G. *Theory of the Stability of Lyophobic Colloids*; Elsevier: New York, 1948.
(15) Reiner, E. S.; Radke, C. J. *J. Chem. Soc., Faraday Trans.* **1990**, *86* (23), 3901.
(16) Feller, S. E.; McQuarrie, D. A. *J. Phys. Chem.* **1992**, *96*, 1354.
(17) Overbeek, J. Th. G. *Colloids Surf.* **1990**, *51*, 61.
(18) Boas, M. L. *Mathematical Methods in the Physical Sciences*; Wiley-Interscience: New York, 1966.
(19) Stigter, D.; Dill, K. A. *J. Phys. Chem.* **1989**, *93*, 6737.

MA9463167